Journal of Oceanology and Limnology
Vol. 40 No. 6, P. 2416-2429, 2022
https://doi.org/10.1007/s00343-022-1375-z

Phytoplankton community dynamics during *Alexandrium* blooms in 2019 off the Qinhuangdao coast, Bohai Sea, China*

Yixuan XIE[1, 2, 3], Renye DING[1, 3], Daojun ZHA[1, 3], Yu LI[1], Guowang YAN[1], Yaya ZHANG[1], Haiyan WU[3], Guanchao ZHENG[3], Zhijun TAN[3, **], Tao JIANG[2, **]

[1] *School of Marine Technology and Geomaties, Jiangsu Ocean University, Lianyungang 222005, China*

[2] *School of Ocean, Yantai University, Yantai 264005, China*

[3] *Key Laboratory of Testing and Evaluation for Aquatic Product Safety and Quality, Ministry of Agriculture and Rural Affairs, Yellow Sea Fisheries Research Institute, Chinese Academy of Fishery Sciences, Qingdao 266071, China*

Received Nov. 9, 2021; accepted in principle Jan. 5, 2022; accepted for publication Apr. 8, 2022

Abstract *Alexandrium* blooms in the northwest area of the Bohai Sea (Qinhuangdao coastal area), China, produce large amounts of toxins that could be enriched in shellfish and consequently harm human bodies. To understand the succession of the phytoplankton community structure during *Alexandrium* bloom events in the northwest area of the Bohai Sea off Qinhuangdao from April 2 to May 7, 2019, microscopy observations and high-performance chromatography (HPLC)-pigment analysis were performed. Sixty species of phytoplankton were identified, mainly diatoms and dinoflagellates. The abundance of *Alexandrium* reached the maximum on April 16 (3.3×10^3 cells/L). HPLC-pigment CHEMTAX analysis showed that the phytoplankton community was composed mainly of diatoms, dinoflagellates, prasinophytes, and cryptophytes. Diatoms were the main contributor to the total Chl-*a* pool. There was a downward trend for the proportion of diatom biomass to the total Chl-*a* pool, followed by an upward trend. The proportion of dinoflagellate biomass showed the opposite trend, whereas that of the prasinophyte biomass presented an obvious increasing trend. Temperature, nutrients, and nutrient structures were the main factors on the distribution of different phytoplankton groups in the study area as shown in the redundancy analysis. This work illustrates the succession of phytoplankton community structures during *Alexandrium* blooms and provided a theoretical basis for studies on the mechanism underlying the outbreak of harmful algal blooms in sea areas.

Keyword: *Alexandrium* bloom; phytoplankton population; environmental factor; high-performance chromatography (HPLC)-CHEMTAX; phytoplankton pigment; Qinhuangdao

1 INTRODUCTION

Phytoplankton is defined as colonies and free-floating unicells that grow photoautotrophically in aquatic environments (Reynolds, 2006). Phytoplankton is an important primary producer given that it fixes more than half of the photosynthetic carbon in the ocean (Pujari et al., 2019). However, under certain environmental conditions, the explosive proliferation or high aggregation of some phytoplankton species results in the ecological abnormality of local discoloration, namely, red tides or harmful algal blooms (HABs). HABs cause harm because the rapid and huge buildup of phytoplankton biomass leads to the depletion of oxygen as the blooms decay or to the destruction of fish or shellfish habitats by the shading of submerged vegetation (Anderson et al., 2002). HABs often cause serious damage to fisheries and mariculture in coastal areas. In addition, toxic algae, including *Alexandrium* spp., can produce biotoxins and seriously threaten the health of consumers throughout the food chain (Costa et al., 2021).

* Supported by the Special Research for the Science and Technology Basic Resources Investigation Program of China (No. 2018FY100200), the National Natural Science Foundation of China (Nos. 31772075, 32072329), and the Project of Jiangsu Natural Science Foundation of China (No. BK20171262)

** Corresponding authors: tanzj@ysfri.ac.cn; jiangtaophy@163.com

Alexandrium blooms have long attracted considerable attention due to their capability to produce highly toxic secondary metabolites, i.e., paralytic shellfish poisoning toxins (PSTs). Among marine biotoxins, PSTs are widely distributed and highly hazardous and have high incidence (Hallegraeff, 1993; Anderson et al., 1996). PSTs are responsible for 87% of global shellfish poisoning incidents, which have a global mortality rate of 2%–14% (Azanza and Taylor, 2001; Raposo et al., 2020). In addition, Paralytic Shellfish Poison (PSP) toxins may be associated with the deaths of birds and humpback whales (Nisbet, 1983; Geraci et al., 1989). Therefore, many countries have listed PSTs as routine detection objects in shellfish farming areas (Nishitani and Chew, 1988; Shumway et al., 1988). *Alexandrium* spp. are important red tide species worldwide, and approximately 10 of these species produce toxins (Hallegraeff, 1993; Dai et al., 2020). Conditions featuring relatively low *Alexandrium* cell densities (>10^3 cells/L) without seawater discoloration are still considered as *Alexandrium* blooms because of their potential threat of PSTs (Anglès et al., 2012). *Alexandrium* bloom outbreaks have been reported in some coastal areas worldwide, including Chile (Jedlicki et al., 2012), Brazil (Persich et al., 2006), the United States (Townsend et al., 2001), Canada (McGillicuddy et al., 2014), the northwestern Mediterranean (Vila et al., 2001), and temperate Asian countries (Yu et al., 2021).

The blooms of *Alexandrium* spp. are rarely monospecific in the natural marine environment. In HABs, *Alexandrium* may dominate the bulk or part of the whole phytoplankton population. For example, *Alexandrium* blooms usually co-occur with the large-scale blooms of *Prorocentrum* spp. in the East China Sea (Zhou et al., 2008; Jiang et al., 2014). Jiang et al. (2014) showed that *Alexandrium tamarense* occupy only a small proportion of the phytoplankton population and that *Prorocentrum* spp. accounts for a large proportion of the spring dinoflagellate blooms in the Nanji Islands. A similar result was also observed in the northwestern Mediterranean, where *Prorocentrum* spp. dominates the phytoplankton community during *Alexandrium* blooms, and other species, such as *Skeletonema costatum* and *Chaetoceros* spp., are present in appreciable numbers (Delgado et al., 1990). *Scrippsiella trochoidea* was the most abundant dinoflagellate species during the *Alexandrium* bloom in the Bay of Plenty, New Zealand, in 1993 (Chang et al., 1997). By contrast, in *Alexandrium* blooms in estuaries in France, *Alexandrium minutum* is the dominant species (60% of the total phytoplankton population) and is accompanied by a small portion of *Nitzschia longissima* (12%) and *Chaetoceros* sp. (23%) (Maguer et al., 2004). In general, the occurrence of *Alexandrium* blooms is a complex process that is affected by complicated environmental factors, under which the phytoplankton population structure is not static and shows variations with time and place.

In most of the previous studies on *Alexandrium* blooms, phytoplankton identification was based on traditional microscopic observation. However, this method is time- and labor-consuming and cannot identify small or fragile algal cells (e.g., picoplankton). Such a constraint leads to biases in the assessment of the changes in phytoplankton population structure during algal blooms. In recent decades, HPLC-pigment-based chemotaxinomic analysis has greatly improved the efficiency of phytoplankton measurement and expanded the understanding of population structure. It has been widely used to reveal the temporal and spatial distributions of the phytoplankton assemblages in nearshore, coastal, and oceanic sea areas (Wright et al., 2010; Zhai et al., 2011; Das et al., 2017; Lu et al., 2018). Short-term changes in algal blooms and phytoplankton communities in some estuary-dominated sea areas under the disturbance of storm events have also been studied by using the HPLC-pigment method (e.g., Jiang et al., 2022). Notably, few studies have been conducted to characterize the succession of phytoplankton communities during the process of *Alexandrium* blooms by using HPLC-pigment analysis.

In the Bohai Sea, the largest inland sea in China, PSP toxins were first detected in *Crassostrea gigas* and *Scapharca subcrenata* in 1996 (Lin et al., 1999). The detection of these toxins signified the possibility of the presence of the PSP-producing genus *Alexandrium* in the seawater. Zhang et al. (2018) reviewed the occurrence of PSP toxins during 1993 to 2016 and suggested that the detection rate and concentration of these toxins in shellfish showed a significant upward trend starting in 2006. However, *Alexandrium* blooms rarely occurred in the Bohai Sea before 2016. For example, only one *Alexandrium* bloom event was observed during 2000 and 2015 (Dou et al., 2020). Nevertheless, the *Alexandrium* genus has been reported to be occasionally the dominant taxon in seawater (Cao et al., 2006; Xu et al., 2017).

Qinhuangdao is located northwest of the Bohai Sea. In recent years, this sea area suffered from a

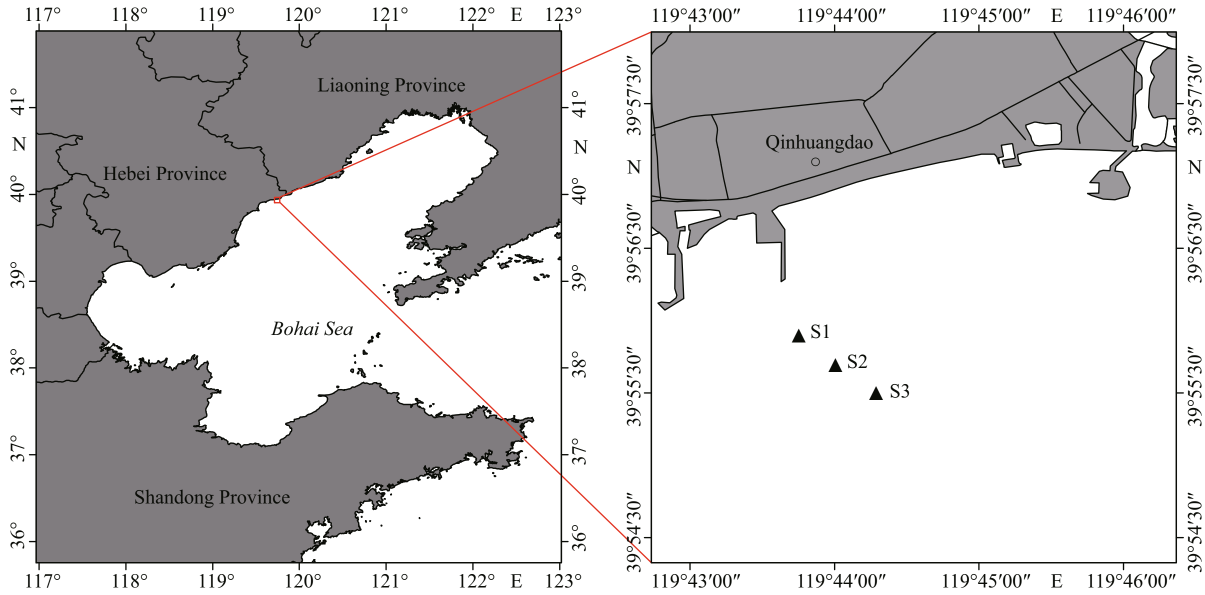

Fig.1 The sampling stations in the Qinghuangdao coastal waters

large amount of land-based pollution sources from industrial, agricultural, and aquaculture wastewaters due to vigorous economic development (Xu et al., 2017; Cui et al., 2018). Consequently, its ecological environment has been deteriorated, and eutrophication in this area was intensified, thus leading to the frequent occurrence of HABs (Peng, 2015; Liu et al., 2017). This area has experienced *Aureococcus anophagefferens* brown tides on an annual basis since 2009 (Xu et al., 2017). These algal blooms have severely affected the development of the local marine economy and attracted widespread concern. Although brown tides have not occurred in this area since 2016, the Qinghuangdao coastal area has experienced high incidences of *Alexandrium* blooms in recent years (Zhang et al., 2018). *Alexandrium* blooms have occurred every spring (in April to May) and resulted in excessive PSP content in shellfish (Ding et al., 2017; Zhang, 2020). An outbreak of PSP poisoning was reported in the spring of 2016. Since then, the local government has issued bulletins every spring on the prevention of paralytic shellfish poisoning because of the recurrence of *Alexandrium* blooms. The annual outbreak of *Alexandrium* blooms has exerted a massive effect on the local shellfish farming industry.

Alexandrium blooms have become a recurring problem in the coastal areas of Qinhuangdao City in recent years. However, the detailed process of *Alexandrium* blooms has yet to be reported. In this study, microscopy examination and HPLC-CHEMTAX pigment analysis were used to track the process of *Alexandrium* blooms in the spring of 2019. The aims of this study are to present the temporal dynamics of phytoplankton assemblages, especially those of *Alexandrium* spp., and to investigate how environmental factors affect the short-term succession of phytoplankton communities in this area in spring.

2 MATERIAL AND METHOD

2.1 Site description and sampling method

Our previous investigations indicated that in the study area, *Alexandrium* blooms mainly occur in April to May (unpublished data). In this study, nine investigations were carried out at three stations in the Qinhuangdao sea area from April 2, 2019 to May 7, 2019 (Fig.1). After May 7, 2019, the cell density of *Alexandrium* decreased to <1 000 cells/L. The sampling stations were approximately 0.8–1.7 km away from the shoreline. Only surface seawater was sampled at shallow water depth (<7 m). Physical parameters, including salinity, temperature, and DO, were measured by using an YSI 556 multiparameter instrument (Yellow Springs Instruments, USA). Seawater samples with an accurate volume of 1.0 L were filtered through GF/F filters (0.7 μm, Whatman). The filters were taken and immediately frozen in liquid nitrogen for pigment analysis. The filtrate was stored at -40 °C in a freezer for the analysis of ammonium nitrogen (NH_4^+), NO_3^-, NO_2^-, DIP, and DSi concentrations. Phytoplankton samples (1.0 L) preserved with acidic Lugol solution were used for microscopy identification.

Table 1 The pigment vs. Chl *a* ratios used in CHEMTAX analysis of pigment data

Class	Peri	But-Fuco	Fuco	Hex-Fuco	Neo	Pras	Viol	Allo	Lut	Zea	Chl *b*	Chl *a*
(a) Initial ratio matrix												
Prasinophytes	0	0	0	0	0.15	0.32	0.06	0	0.01	0	0.95	1
Dinoflagellates	1.06	0	0	0	0	0	0	0	0	0	0	1
Cryptophytes	0	0	0	0	0	0	0	0.23	0	0	0	1
Haptophytes	0	0.02	0.05	1.20	0	0	0	0	0	0	0	1
Chlorophytes	0	0	0	0	0.06	0	0.06	0	0.20	0.01	0.26	1
Diatoms	0	0	0.75	0	0	0	0	0	0	0	0	1
Cyanobacteria	0	0	0	0	0	0	0	0	0	1.20	0	1
Chrysophytes	0	1.30	0.20	0.01	0	0	0	0	0	0	0	1
(b) Final ratio matrix												
Prasinophytes	0	0	0	0	0.13	0.33	0.07	0	0.01	0	0.93	1
Dinoflagellates	1.01	0	0	0	0	0	0	0	0	0	0	1
Cryptophytes	0	0	0	0	0	0	0	0.22	0	0	0	1
Haptophytes	0	0.02	0.05	1.19	0	0	0	0	0	0	0	1
Chlorophytes	0	0	0	0	0.06	0	0.05	0	0.18	0.01	0.31	1
Diatoms	0	0	0.75	0	0	0	0	0	0	0	0	1
Cyanobacteria	0	0	0	0	0	0	0	0	0	1.14	0	1
Chrysophytes	0	1.30	0.21	0.01	0	0	0	0	0	0	0	1

2.2 Nutrient analysis

The concentrations of NH_4^+ , NO_3^- , NO_2^-, and dissolved inorganic phosphate (PO_4^-) and metasilicate (SiO_3^-) were measured by using a Skalar San^{++} continuous flow analyzer (Strickland and Parsons, 1972). DIN refers to the sum of NO_3^-, NO_2^-, and NH_4^+ contents.

2.3 HPLC pigment analysis

Photosynthetic pigments were extracted in darkness and low temperature as per Lu et al. (2018). HPLC analysis was performed as per Zapata et al. (2000) by using an Agilent series 1100 HPLC system equipped with a G1314A detector and Waters Symmetry C8 column (150×4.6 mm, 3.5-μm particle size, 100-Å pore size). The absorption spectrum at 440 nm and the peak time were used to identify the pigment peak, and the retention times were compared with the retention times of the authentic standards obtained from DIH Inc. (Hørsholm, Denmark). The relative standard deviation for pigment analysis was controlled within ±5%. A total of 22 standards were used. They included chlorophyll *c3*, Mg-2,4-divinylpheopor-phyrin, chlorophyll *c2*, peridinin (Peri), pheophorbide *a* (Pheide *a*), 19-but-fucoxanthin (But-Fuco), fucoxanthin (Fuco), neoxanthin (Neo), prasinoxanthin (Pras), violaxanthin (Viol), 19′-hex-fucoxanthin (Hex-Fuco), diadinoxanthin, alloxanthin (Allo), diatoxanthin, zeaxanthin (Zea), lutein (Lut), canthaxanthin, gyroxanthin-diester, chlorophyll *b* (Chl *b*), chlorophyll *a* (Chl *a*), pheophythin *a* (Phe *a*), and β-carotene (β-Car).

2.4 CHEMTAX analysis

Version 1.95 of CHEMTAX software was used to calculate the contributions of different phytoplankton groups to total Chl *a*. The initial pigment ratio matrix was derived from a series of values given by Mackey et al. (1996). The initial and output matrixes are shown in the appendix as Table 1. Each cell of the initial matrix was multiplied with a random function to generate a series of 60 derivative pigment ratio matrixes. The macro was applied to calculate the best six output results, and the average was taken.

2.5 Phytoplankton identification and enumeration

The sample was concentrated to a volume of 10–20 mL after 48 h of precipitation. Identification and counting were performed under an inverted microscope in accordance with Utermöhl (1958). The references used for the identification of phytoplankton species included Illustrations of Common Planktonic Diatoms in Chinese Seas by Yang and Dong (2006), Dinoflagellates in China's Seas III (Peridiniales) by Yang et al. (2019), and Illustrations of Plankton Responsible for the Blooms in Chinese Coastal Waters by Guo (2004).

2.6 Statistical analysis

The Pearson analysis was conducted by using SPSS Statistics (version 23) to test the correlation between the microscopy observation data and CHEMTAX results. Redundancy analysis (RDA) was performed with CANOCO 5 software to explore the relationships between environmental and biological (phytoplankton) variables.

Species diversity, ecological richness, species evenness, and dominance indexes were used to evaluate the diversity of the phytoplankton community structure. The main formulas are given below.

The Shannon-Wiener diversity index was used as the species diversity index (H') and is calculated as

$$H' = \sum_{i=1}^{n} P_i \log_2 P_i. \quad (1)$$

The Makarev index was utilized as the ecological richness index (d_{Ma}) and has the formula:

$$d_{\mathrm{Ma}} = \frac{S-1}{\ln N}. \quad (2)$$

The Pielou index was applied as the species evenness index (J) and is given as

$$J = \frac{H'}{\log_2 S}. \quad (3)$$

The dominance index of phytoplankton (Y) is

$$Y = \frac{n_i}{N} f_i, \quad (4)$$

where N represents the total number of individuals; P_i represents the ratio of the individual number of the i^{th} species in a sample to the individual number of the sample; S represents the total number of species in a sample; n_i represents the total number of individuals of the i^{th} species; and f_i represents the frequency of the occurrence of the i^{th} species in each sample. The dominant species are those whose dominance degrees exceeded 0.02.

3 RESULT

3.1 Physical and chemical parameters

The sampling time for this survey was set at 9:00–11:00 am each time and did not take tidal effects into account. During the survey period, the sea surface temperature continued to increase from 6.8 °C to 14.2 °C (Fig.2a). Salinity remained very stable and ranged from 32.0 to 32.2. Although the DO concentration showed a downward trend, hypoxia (<3.0 mg/L) did not occur. The average concentrations of DIN, DIP, and DSi were 2.9, 0.2, and 2.6 μmol/L, respectively. During the investigation period, the concentrations of DIN and DIP showed a downward trend, whereas the concentration of DSi exhibited an upward trend (Fig.2b). The potential Si limit appeared during April 2–16 when the DIN/DSi ratio ranged from 2.08 to 2.89 and the DSi/DIP ratio was less than 11.58 (Fig.2d). However, after April 19, DIP concentration decreased to less than 0.1 μmol/L, and the ratios of DIN/DIP and DSi/DIP increased to 30, thus indicating P limitation (Fig.2b & c) (Dortch and Whitledge, 1992). The concentration of NO_2^- was relatively stable and ranged from 0.18 μmol/L to 0.31 μmol/L (Fig.2c). NO_3^- concentration decreased from 1.7 μmol/L to 0.05 μmol/L, and NH_4^+ concentration decreased from 3.36 μmol/L to 1.28 μmol/L, with both indexes generally showing a downward trend (Fig.2c).

3.2 Phytoplankton pigment concentrations

A total of 17 pigments were identified. They included Peri, Pheide *a*, But-Fuco, Fuco, Neo, Pras, Viola, Hex-Fuco, Diad, Allo, Diat, Zea, Lut, Chl *b*, Chl *a*, Phe *a*, and β-Car. Fuco, followed by Chl *a*, and Peri, was the most abundant. The concentration of Chl *a* remained relative high (>0.62 μg/L) before April 16, decreased sharply to 0.24 μg/L on April 19, and then presented an increasing trend (Fig.3a). The average concentration of Fuco reached 0.69 μg/L and showed a change trend that was similar to that exhibited by the concentration of Chl *a*. By contrast, Peri concentration increased before April 19 and then decreased with an average value of 0.20 μg/L (Fig.3a). The average concentrations of Chl *b*, Pras, and Zea were 0.07, 0.11, and 0.005 μg/L, respectively. Pras concentration showed an upward trend during the investigation period (Fig.3b).

3.3 Phytoplankton community structure based on CHEMTAX

CHEMTAX analysis revealed the variation in the composition of the phytoplankton community during the study period. Diatoms, dinoflagellates, prasinophytes, and cryptophytes were the main phytoplankton groups in the study area, whereas chlorophytes, haptophytes, cyanobacteria, and chrysophytes accounted for a low proportion of the

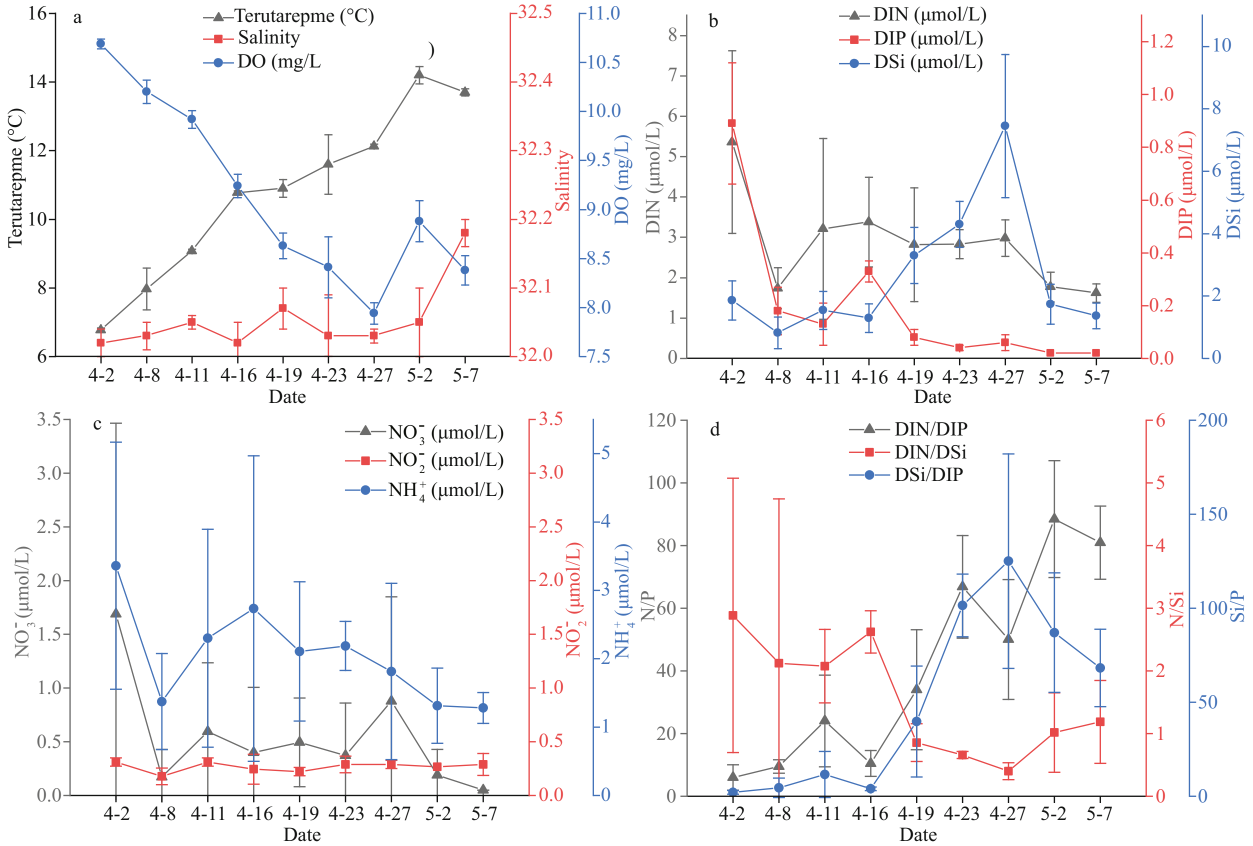

Fig.2 Values of the environmental factors of the Qinghuangdao coastal waters in spring

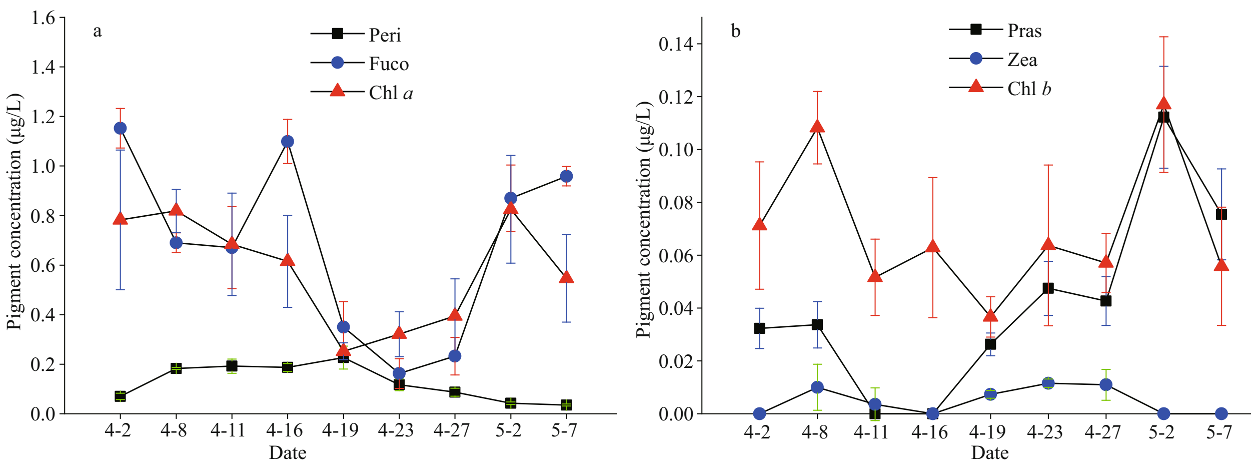

Fig.3 Temporal distribution of the main pigments in the Qinghuangdao coastal waters in spring

total phytoplankton biomass (Fig.4). The CHEMTAX-derived diatom biomass accounted for the highest percentage of the total biomass (43.1% of Chl *a* on average). The proportion of diatom biomass showed an upward trend after decreasing, whereas that of the dinoflagellate biomass presented the opposite trend (Fig.4). Prasinophyte biomass was low (<0.11-μg/L Chl *a*) before April 19 and gradually increased to the maximum value of 0.30 μg/L Chl *a* in the late stage of the algal bloom (Fig.4a). On average, chlorophytes, haptophytes, cyanobacteria, and chrysophytes accounted for only 13.8%, 0.7%, 1.1%, and 2.1% of the biomass, respectively (Fig.4b).

3.4 Phytoplankton community structure based on microscopy observation

A total of 60 algal species were identified via microscopy observation. These species belonged to three phytoplankton groups: diatoms, dinoflagellates, and chrysophytes. The microscopy results showed

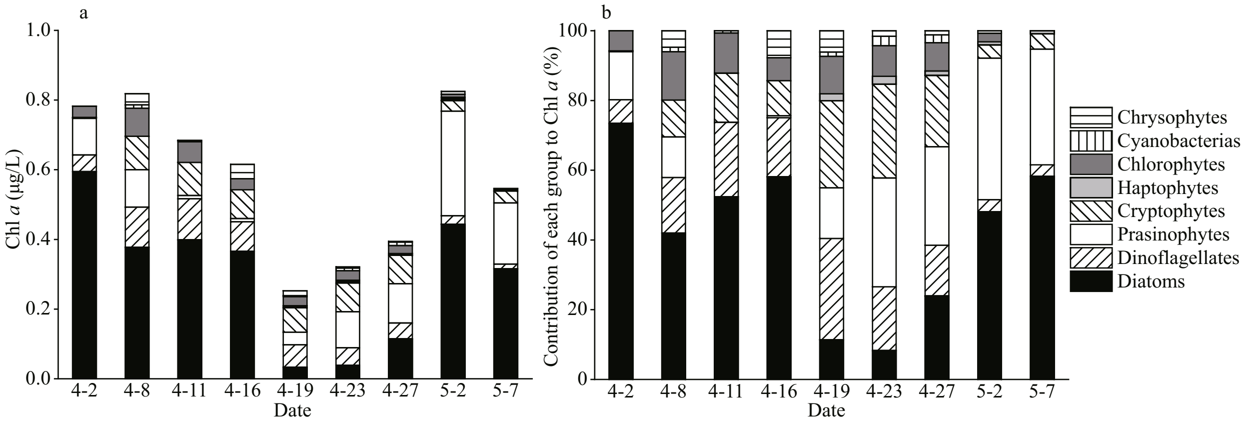

Fig.4 Contributions of various phytoplankton functional groups to Chl *a* and various phytoplankton biomasses in the Qinghuangdao coastal waters in spring

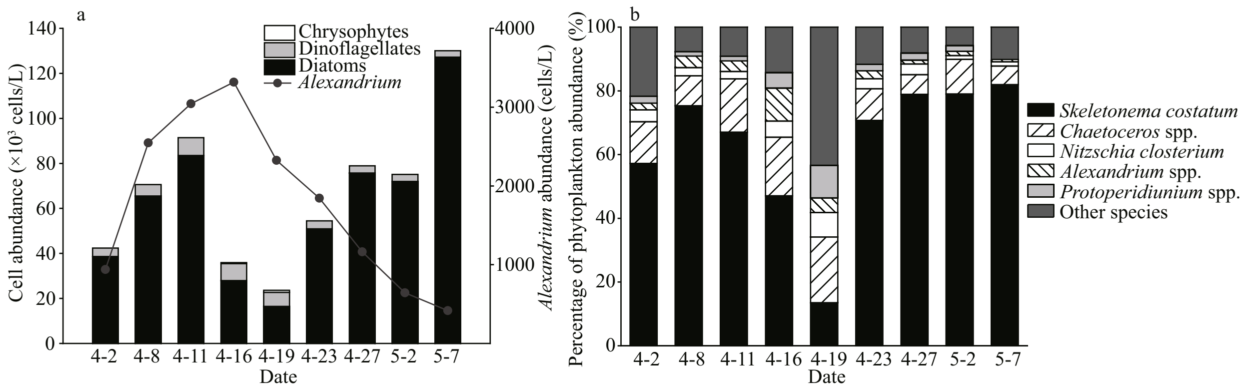

Fig.5 The cell abundances of phytoplankton in the Qinghuangdao coastal waters in spring based on microscopy observations

that the total phytoplankton abundance ranged from 23.0×10^3 cells/L to 130.1×10^3 cells/L (Fig.5a). The phytoplankton community was mainly composed of diatoms (71.7%–97.8%) and dinoflagellates (2.2%–27.0%). The abundance of diatoms increased at first before April 11 and then decreased until April 19. Finally, it increased gradually. By contrast, the abundance of dinoflagellates first increased and then decreased. Chrysophytes were detected with low cell abundances (≤3.8% of the total phytoplankton abundance) on April 16 and 19 (Fig.5a).

The dominant species were *Skeletonema costatum*, *Chaetoceros* spp., *Nitzschia closterium*, *Alexandrium* spp., and *Protoperidiunium* spp. *S. costatum* was the first dominant species. It accounted for 69.6% of the total phytoplankton cells on average (Fig.5b). *Chaetoceros* spp. was the second dominant genus (11.5% on average). Its abundance first increased and then decreased (Fig.5b). *Alexandrium* spp. (2.6% on average) and *Protoperidiunium* spp. (2.1% on average) were the two dominant dinoflagellate genera (Table 2). The abundance of *Alexandrium* spp. continued to increase during the pre-bloom period. It reached the maximum value of 3.3×10^3 cells/L on April 16 and

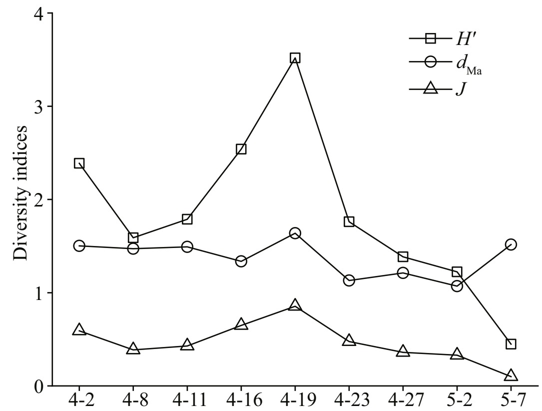

Fig.6 Diversity indexes of the phytoplankton community in the Qinghuangdao coastal waters in spring

then decreased to 0.4×10^3 cells/L on May 7 (Fig.5a).

H' (0.44–3.52), d_{Ma} (1.07–1.64), and J (0.10–0.85) reached their maximum values on April 19 (Fig.6). H' and J increased before April 19 and then decreased to their lowest values on May 7 (Fig.6).

3.5 Comparison of cell counts and CHEMTAX estimates

The CHEMTAX-derived Chl *a* estimates and

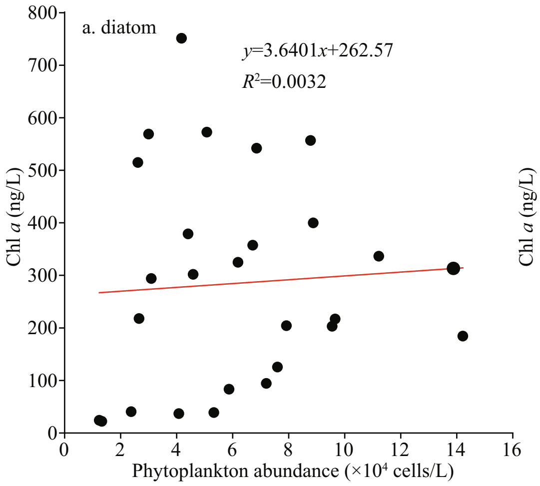

Fig.7 Linear relationship of the phytoplankton abundances obtained through microscopy cell counting with the CHEMTAX-derived biomass (* P<0.05)

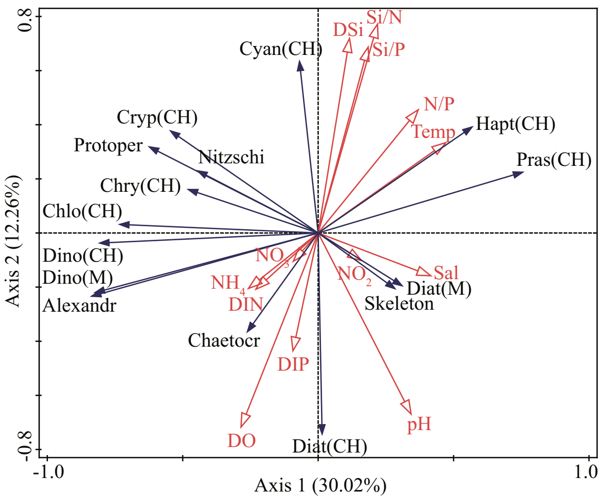

Fig.8 RDA ordination plots showing the relationships of phytoplankton species with environmental variables in the Qinghuangdao coastal waters

M: microscopy results; CH: CHEMTAX results; temp: temperature; sal: salinity; Pras: prasinophytes; Din: dinoflagellates; Crypt: cryptophytes; Hapt: haptophytes; Chlor: chlorophytes; Diat: diatoms; Cyan: cyanobateria; Chrys: chrysophytes; Skeleton: *Skeletonema costatum*; Chaetoce: *Chaetoceros* spp.; Nitzschi: *Nitzschia closterium*; Alexandr: *Alexandrium* spp.; Protoper: *Protoperidiunium* spp.

phytoplankton cell abundances were compared. Statistical analysis showed that the algal cell abundance and CHEMTAX estimates for diatoms were not significantly correlated (P>0.05; Fig.7). The microscopy counting results and CHEMTAX estimates for dinoflagellates were significantly correlated (P<0.05).

3.6 Effects of environmental factors on phytoplankton community structure

RDA was conducted to investigate the correlation between phytoplankton and environmental factors (Fig.8). The cumulative contribution of the first two axes to the relationship between species and the environment was 72.14%. RDA showed that *Alexandrium* was negatively correlated with temperature. Diatom cell density was positively correlated with salinity and pH. Dinoflagellate cell density was positively correlated with NH_4^+, DIN, and DIP and negatively correlated with temperature. The Chl-*a* values of diatoms were positively correlated with DIP and negatively correlated with DSi, N/P, Si/N, and Si/P. The Chl-*a* values of dinoflagellates, chlorophytes, and chrysophyta were positively correlated with DIN and negatively correlated with DSi, N/P, Si/N, and Si/P. Temperature and salinity were the main environmental factors affecting cryptophytes and haptophytes (Fig.8).

4 DISCUSSION

4.1 Dynamics of *Alexandrium* spp. in the Qinghuangdao sea area

Two conditions are needed for the formation of HABs: an algal density exceeding 10^5 or 10^6 cells/L and water discoloration (Anderson, 2014). However, events wherein the density of toxic algae (e.g., *Alexandrium* spp.) is low are considered as algal blooms in consideration of environmental safety, especially food safety. In the Gulf of Maine, shellfish harvest is banned when *Alexandrium* concentrations reach 100 cells/L to prevent paralytic toxin poisoning (Wells et al., 2020). In this study, *Alexandrium* spp. dinoflagellates in seawater samples were observed under microscopy but could not be accurately

Table 2 Dominant species of phytoplankton in the Qinghuangdao coastal waters in spring

Species of phytoplankton	Abundance ratio (%)	Dominance degree
Skeletonema costatum	69.6	0.696
Chaetoceros spp.	11.5	0.115
Nitzschia closterium	2.7	0.027
Alexandrium spp.	2.6	0.026
Protoperidiunium spp.	2.1	0.021

identified. Previous investigations have suggested that *A. catenella* and *A. pacificum* are the most likely causative species of poisoning outbreaks in the Qinhuangdao coastal area (Gao et al., 2015; Yu et al., 2021). A parallel experiment conducted by Zhang (2020) revealed that the toxin content in mussels is highly consistent with the abundance of *Alexandrium* cells in this area. For example, the highest density of *Alexandrium* was 3.3×10^3 cells/L (on April 16) (Fig.5a), and the PSP content in mussels reached the highest value (929 µg STXeq/kg meat, exceeding the regulation limit of 800 µg STXeq/kg meat) during the whole investigation period (Zhang, 2020). Consequently, in the present study, the minor intrusion of an undesirable species (i.e., genus *Alexandrium*) into the common phytoplankton community was considered as an *Alexandrium* bloom event (Wells et al., 2020).

In this study, *Alexandrium* spp. showed good growth potential at 8.0–11.0 °C. Regression analysis revealed that the highest cell abundance of *Alexandrium* spp. appeared at approximately 10 °C (Fig.9). Similarly, the highest cell densities were observed at 8–9 °C in Oppa Bay (Ichimi et al., 2001). In addition, the temperature associated with the highest cell density was higher in some sea areas than in Qinhuangdao. For example, the maximum cell density of *Alexandrium* in Northport-Huntington Bay and the southern coast of Korea was observed at approximately 15 °C (Hattenrath et al., 2010; Kim et al., 2020). The highest cell densities of *Alexandrium minutum* were observed in the Penze Estuary (France) at 16.3–18.9 °C (Maguer et al., 2004). The small variations in salinity (32.00–32.20) suggested that in the study area, temporal variation was less influenced by salinity than by other factors (Figs.2a & 8).

Nutrient concentration and structure are also important factors that influence the dynamics of *Alexandrium* in nearshore and coastal areas (Hattenrath et al., 2010; Jiang et al., 2014). An investigation in Northport by Hattenrath et al.

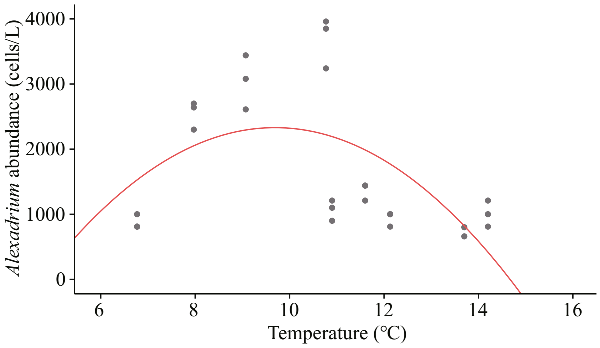

Fig.9 Curve fitting of *Alexandrium* cell abundance with the temperature in the Qinhuangdao sea area

(2010) showed that N input from sewage effluent plays an important role in the development and toxicity of *Alexandrium fundyense* blooms. Among different N components, NH_4^+ may be the most effective in increasing the density of *A. fundyense* (Hattenrath et al., 2010). Our results showed that NH_4^+ concentration was higher than NO_3^- and NO_2^- concentrations (Fig.2c) with the former seeming to have a greater effect on *Alexandrium* than the latter as shown by RDA (Fig.8). However, the abundance of *Alexandrium* spp. decreased gradually when DIP limitation (<0.1 µmol/L) occurred, and the ratios of DIN/DIP and DSi/DIP increased to 30 starting on April 19 (Figs.2 & 5). Previous studies suggested that *Alexandrium* spp. are poorer phosphorus competitors than other algal species (Jiang et al., 2014). RDA further corroborated the above conclusions by demonstrating that *Alexandrium* spp. had a positive correlation with dissolved inorganic nitrogen and phosphate (Fig.8). Similar results were observed in the sea areas of the Nanji Islands, where *A. tamarense* blooms are terminated by low DIP concentrations (<0.1 µmol/L) (Jiang et al., 2014). In summary, we suggest that NH_4^+ has a great effect on *Alexandrium* blooms, whereas DIP limitation may be responsible for the collapse of *Alexandrium* blooms. Moreover, dissolved organic nitrogen (DON) may play an important role in supporting *Alexandrium* blooms (Hattenrath et al., 2010). This role, however, was not quantified in this study. Future studies should pay further attention to DON concentrations because they may stimulate the blooms of *A. anophagefferens* in the Qinhuangdao coastal areas (Ou et al., 2018).

4.2 Temporal variability in phytoplankton assemblages and related influencing factors in spring

Previous results have suggested that the abundance of dinoflagellates along the coastal areas of

Qinhuangdao often peak in spring (Chen et al., 2016; Xu et al., 2017). In this study, microscopy observation revealed that in the study period, diatoms and dinoflagellates coexisted; however, the former was more dominant than the latter (Fig.5; Table 2). One reasonable explanation for this phenomenon is that dinoflagellates generally exhibit slower growth rates than diatoms, and the latter can apparently outcompete dinoflagellates even when silicate decreases to near-limiting concentrations in late spring (Grenney et al., 1973; Parsons et al., 1978). The dominant diatom taxa, i.e., *Skeletonema* spp. (warm-water species) and *Chaetoceros* spp. (oceanic species), have rapid growth rates and can quickly exploit available resources and dominate the phytoplankton community (Banse, 1982; Yang et al., 1996). Thus, diatoms can apparently still outgrow and outcompete dinoflagellates even when silicate decreases to near-limiting concentrations in the late spring and early summer (Grenney et al., 1973; Parsons et al., 1978).

The comparison of algal cell abundance and CHEMTAX biomass revealed a significant positive correlation only for dinoflagellates but not for diatoms (Fig.7). Only two dinoflagellate taxa, i.e., *Alexandrium* spp. and *Protoperidiunium* spp., coexisted in the seawater (Fig.5b) and showed similar cell sizes (approximately 18–31 μm). By contrast, the species number of diatoms was considerably larger than that of dinoflagellates (Fig.5a), and the cell sizes of different diatom taxa were quite different (Pan et al., 2020). The latter may be the key reason for the nonsignificant linear correlation between the cell abundance and CHEMTAX biomasses of diatoms. The omission of small diatoms by microscopy was another influencing factor (Agirbas et al., 2015).

Small nondiatoms can be regarded as the background component of the planktonic community that is responsible for the recycling of organic matter within the euphotic layer (Seoane et al., 2011). However, some algal species, such as cryptophytes, cyanobacteria, and prasinophytes, are often neglected in microscopy observation due to the limitations of the method. This study showed that HPLC-pigment CHEMTAX is a suitable tool for assessing the composition and biomass of phytoplankton groups in the Qinhuangdao sea area. To the best of our knowledge, the CHEMTAX analysis of the phytoplankton community in this area has yet to be reported. Our results confirmed that prasinophytes, chlorophytes, and cryptophytes substantially contributed to the total Chl-*a* pool; these results were not observed via microscopy (Figs.4–5). The combination of microscopy and HPLC-pigment CHEMTAX highlighted the complementary advantages of the two methods in studies on algal blooms.

The present study showed through microscopy and HPLC analyses that the phytoplankton community changed obviously in just 36 days (Figs.3–5). Several physicochemical variables, such as temperature, salinity, and nutrient availability and structure, influence the temporal variations in phytoplankton communities (Álvarez-Góngora and Herrera-Silveira, 2006; Hunt et al., 2010). These changes confirmed that the phytoplankton community structure in the Qinhuangdao coast was not invariable in spring. This variability might be a reflection of the complex interplay between different phytoplankton taxa and other abiotic and biotic factors (Kremp et al., 2009). Considering this phenomenon, representing the seasonal variations in phytoplankton community structure through a single sampling event in spring may result in deviations from the results of previous studies (e.g., Lu et al., 2018; Wang et al., 2018; Miranda-Alvarez et al., 2020).

The rapid increment in seawater temperature in the spring (Fig.2a) may be an important environmental parameter that affects marine biological processes (Cui et al., 2018; Lu et al., 2018; Pan et al., 2020). Previous studies have suggested that temperature could induce changes with a regular and predictable pattern in phytoplankton community structure (Mendes et al., 2015; Pan et al., 2020). In general, diatoms usually flourish at low temperatures in nearshore areas (<18 °C) (Wasmund et al., 2011; Pan et al., 2020). In this study, the seawater temperature was low (<14.2 °C), and diatoms and temperature were not closely correlated (Fig.8). The significant increase in the proportion of prasinophytes and haptophytes in the total phytoplankton biomass with temperature was a prominent phenomenon (Figs.4 & 8). Similarly, Lu et al. (2018) reported that in the central Bohai Sea, phytoplankton assemblages transition from diatom-dominated in spring to flagellate-dominated (mainly haptophytes and prasinophytes) in early summer. Thus, temperature rise might be the key factor promoting the growth of prasinophytes and haptophytes in the sea area under study, as well as in the central Bohai Sea (Pan et al., 2020; Yan et al., 2020).

Nutrient concentration and structure are other important factors affecting the species composition and biomass of phytoplankton in the marine environment (Zhang et al., 2004; Xu et al., 2010; Pei et al., 2019). Given that different phytoplankton taxa have different nutrient demands and uptake capabilities, nutrient imbalance or limitation is an important reason for the poverty of some phytoplankton taxa or the changes in community composition (Xu et al., 2010). Usually, nutrient-enriched coastal waters support the growth of large phytoplankton, e.g., diatoms and dinoflagellates (Sarthou et al., 2005; Lionard et al., 2008). Similarly, our results showed that diatoms and dinoflagellates were the main phytoplankton assemblages when DIN and DIP were high on April 19 (Figs.4 & 5). This result was further confirmed by RDA, which revealed a positive correlation between dinoflagellates (microscopy counts and CHEMTAX estimates) and diatoms (CHEMTAX estimates), as well as DIN and DIP concentrations (Fig.8). Prasinophytes have a broad capability to respond to nutrient variations (Not et al., 2004). In this study, the negative association of prasinophyte biomass with DIN and DIP (Fig.8) suggested that nutrient concentration was not the factor that stimulated their increase in the study area. By contrast, the positive correlation of the CHEMTAX-estimated biomasses of chlorophytes and cryptophytes with DIN implied that DIN played an important role in the growth of these taxa. Moreover, although DSi concentration is an important factor that affects the growth of diatoms in some coastal areas (Drira et al., 2014; Erga et al., 2014), in this study, diatom biomass was not positively related to DSi concentration (Fig.8). This result indicated that DSi concentration was not a limiting factor of the diatoms in this sea area.

5 CONCLUSION

This study investigated the occurrence of the low-density blooms of *Alexandrium* spp. in the Qinhuangdao coastal area in spring of 2019. The highest abundance of *Alexandrium* spp. was 3.3×10^3 cells/L and was observed at approximately 10 °C. *Alexandrium* spp. density gradually decreased starting on April 19 upon DIP limitation. It is important to note that even at low density and low Chl-*a* concentration, *Alexandium* bloom could cause serious harmfulness, which might be ignored in HAB monitoring. The temporal succession of the phytoplankton community during the period of *Alexandrium* blooms was revealed by using microscopy and HPLC. In addition to the predominant diatoms and dinoflagellates, small nondiatoms (i.e., cryptophytes, cyanobacteria, and prasinophytes) substantially contributed to the total Chl-*a* pool during the investigation. This study further demonstrated the importance of the combination of microscopy cell counting and CHEMTAX estimation for the investigation of phytoplankton communities. The temporal variations in phytoplankton assemblages were most likely influenced by temperature and nutrient availability. Increases in temperature promoted the growth of prasinophytes and haptophytes. The concentrations of DIN, of which NH_4^+ was the most influential, and DIP affected the succession of diatoms and dinoflagellates. Consequently, further attention should be paid to the short-term changes in phytoplankton communities to improve the understanding of the laws governing the temporal variabilities of phytoplankton assemblages in the Bohai Sea.

6 DATA AVAILABILITY STATEMENT

The datasets generated and/or analyzed during the current study are available from the corresponding author on reasonable request.

7 ACKNOWLEDGMENT

The authors would like to thank Mr. Liqiang FAN and Mrs. Qianqian GENG from Key Laboratory of Testing and Evaluation for Aquatic Product Safety and Quality, Ministry of Agriculture and Rural Affairs, Yellow Sea Fisheries Research Institute, Chinese Academy of Fishery Sciences, Qingdao 266071, China, for assistance in field investigation and sample analysis.

References

Agirbas E, Feyzioglu A M, Kopuz U et al. 2015. Phytoplankton community composition in the south-eastern Black Sea determined with pigments measured by HPLC-CHEMTAX analyses and microscopy cell counts. *Journal of the Marine Biological Association of the United Kingdom*, **95**(1): 35-52, https://doi.org/10.1017/S002531541401040.

Álvarez-Góngora C, Herrera-Silveira J A. 2006. Variations of phytoplankton community structure related to water quality trends in a tropical karstic coastal zone. *Marine Pollution Bulletin*, **52**(1): 48-60, https://doi.org/10.1016/j.marpolbul.2005.08.006.

Anderson D M, Glibert P M, Burkholder J M. 2002. Harmful algal blooms and eutrophication: nutrient sources, composition, and consequences. *Estuaries*, **25**(4): 704-726, https://www.researchgate.net/publication/225519007.

Anderson D M, Kulis D M, Qi Y Z et al. 1996. Paralytic shellfish poisoning in southern China. *Toxicon*, **34**(5): 579-590, https://doi.org/10.1016/0041-0101(95)001581.

Anderson D. 2014. HABs in a changing world: a perspective on harmful algal blooms, their impacts, and research and management in a dynamic era of climactic and environmental change. *Harmful Algae 2012*, **2012**: 3-17.

Anglès S, Garcès E, Reñé A et al. 2012. Life-cycle alternations in *Alexandrium minutum* natural populations from the NW Mediterranean Sea. *Harmful Algae*, **16**: 1-11, https://doi.org/10.1016/j.hal.2011.12.006.

Azanza R V, Taylor F J R M. 2001. Are *Pyrodinium* blooms in the Southeast Asian region recurring and spreading? A view at the end of the millennium. *Ambio*: *A Journal of the Human Environment*, **30**(6): 356-364, https://doi.org/10.1579/0044-7447-30.6.356.

Banse K. 1982. Cell volumes, maximal growth rates of unicellular algae and ciliates, and the role of ciliates in the marine pelagial. *Limnology and Oceanography*, **27**(6): 1059-1071, https://doi.org/10.4319/lo.1982.27.6.1059.

Cao C H, Sun Z N, Wang X K et al. 2006. Preliminary study on net-phytoplankton community structure and red tide causative species in Tianjin Sea Area, Bohai Sea. *Journal of Tianjin University of Science & Technology*, **21**(3): 34-37. (in Chinese with English abstract)

Chang F H, Anderson D M, Kulis D M et al. 1997. Toxin production of *Alexandrium minutum* (Dinophyceae) from the Bay of Plenty, New Zealand. *Toxicon*, **35**(3): 393-409, https://doi.org/10.1016/S0041-0101(96)00168-7.

Chen Y H, Gao Y H, Chen C P et al. 2016. Seasonal variations of phytoplankton assemblages and its relation to environmental variables in a scallop culture sea area of Bohai Bay, China. *Marine Pollution Bulletin*, **113**(1-2): 362-370, https://doi.org/10.1016/j.marpolbul.2016.10.025.

Costa A, Alio V, Sciortino S et al. 2021. Algal blooms of *Alexandrium* spp. and paralytic shellfish poisoning toxicity events in mussels farmed in Sicily. *Italian Journal of Food Safety*, **10**(1): 9062, https://doi.org/10.4081/ijfs.2021.9062.

Cui L, Lu X X, Dong Y L et al. 2018. Relationship between phytoplankton community succession and environmental parameters in Qinhuangdao coastal areas, China: a region with recurrent brown tide outbreaks. *Ecotoxicology and Environmental Safety*, **159**: 85-93, https://doi.org/10.1016/j.ecoenv.2018.04.043.

Dai L, Yu R C, Geng H X et al. 2020. Resting cysts of *Alexandrium catenella* and *A. pacificum* (Dinophyceae) in the Bohai and Yellow Seas, China: abundance, distribution and implications for toxic algal blooms. *Harmful Algae*, **93**: 101794, https://doi.org/10.1016/j.hal.2020.101794.

Das S K, Routh J, Roychoudhury A N et al. 2017. Connecting pigment composition and dissolved trace elements to phytoplankton population in the southern Benguela upwelling zone (St. Helena Bay). *Journal of Marine Systems*, **176**: 13-23, https://doi.org/10.1016/j.jmarsys.2017.07.009.

Delgado M, Estrada Miyares M, Camp J et al. 1990. Development of a toxic *Alexandrium minutum* Halim (Dinophyceae) bloom in the Harbour of Sant Carles de la Ràpita (Ebro Delta, northwestern Mediterranean). *Scientia Marina*, **54**(1): 1-7.

Ding L, Qiu J B, Li A F. 2017. Proposed biotransformation pathways for new metabolites of paralytic shellfish toxins based on field and experimental mussel samples. *Journal of Agricultural and Food Chemistry*, **65**(27): 5494-5502, https://doi.org/10.1021/acs.jafc.7b02101.

Dortch Q, Whitledge T E. 1992. Does nitrogen or silicon limit phytoplankton production in the Mississippi River plume and nearby regions? *Continental Shelf Research*, **12**(11): 1293-1309, https://doi.org/10.1016/0278-4343(92)90065-R.

Dou Y, Shang J S, Shao P et al. 2020. Frequency of red tides in Bohai Sea and the influence of environmental factors (2000-2016). *Journal of Hydroecology*, **41**(6): 141-148. (in Chinese with English abstract)

Drira Z, Elloumi J, Guermazi W et al. 2014. Seasonal changes on planktonic diatom communities along an inshore-offshore gradient in the Gulf of Gabes (Tunisia). *Acta Ecologica Sinica*, **34**(1): 34-43, https://doi.org/10.1016/j.chnaes.2013.11.005.

Erga S R, Ssebiyonga N, Hamre B et al. 2014. Nutrients and phytoplankton biomass distribution and activity at the Barents Sea Polar Front during summer near Hopen and Storbanken. *Journal of Marine Systems*, **130**: 181-192, https://doi.org/10.1016/j.jmarsys.2012.12.008.

Gao Y, Yu R C, Chen J H et al. 2015. Distribution of *Alexandrium fundyense* and *A. pacificum* (Dinophyceae) in the Yellow Sea and Bohai Sea. *Marine Pollution Bulletin*, **96**: 210-219, https://doi.org/10.1016/j.marpolbul.2015.05.025.

Geraci J R, Anderson D M, Timperi R J et al. 1989. Humpback whales (*Megaptera novaeangliae*) fatally poisoned by dinoflagellate toxin. *Canadian Journal of Fisheries and Aquatic Sciences*, **46**(11): 1895-1898, https://doi.org/10.1139/f89-238.

Grenney W J, Bella D A, Curl H C Jr. 1973. A theoretical approach to interspecific competition in phytoplankton communities. *American Naturalist*, **107**(955): 405-425.

Guo H. 2004. Illustrations of Planktons Responsible for the Blooms in Chinese Coastal Waters. China Ocean Press, Beijing, China. 107p. (in Chinese)

Hallegraeff G M. 1993. A review of harmful algal blooms and their apparent global increase. *Phycologia*, **32**(2): 79-99, https://doi.org/10.2216/i0031-8884-32-2-79.1.

Hattenrath T K, Anderson D M, Gobler C J. 2010. The influence of anthropogenic nitrogen loading and meteorological conditions on the dynamics and toxicity of *Alexandrium fundyense* blooms in a New York (USA) estuary. *Harmful Algae*, **9**(4): 402-412, https://doi.org/10.1016/j.hal.2010.02.003.

Hunt C D, Borkman D G, Libby P S et al. 2010. Phytoplankton patterns in Massachusetts Bay 1992-2007. *Estuaries and Coasts*, **33**(2): 448-470, https://doi.org/10.1007/s12237-008-9125-9.

Ichimi K, Yamasaki M, Okumura Y et al. 2001. The growth and cyst formation of a toxic dinoflagellate, *Alexandrium tamarense*, at low water temperatures in northeastern Japan. *Journal of Experimental Marine Biology and Ecology*, **261**(1): 17-29, https://doi.org/10.1016/S0022-0981(01)00256-8.

Jedlicki A, Fernández G, Astorga M et al. 2012. Molecular detection and species identification of *Alexandrium* (Dinophyceae) causing harmful algal blooms along the

Chilean coastline. *AoB Plants*, **2012**: pls033, https://doi.org/10.1093/aobpla/pls033.

Jiang T, Wu G N, Niu P L et al. 2022. Short-term changes in algal blooms and phytoplankton community after the passage of Super Typhoon Lekima in a temperate and inner sea (Bohai Sea) in China. *Ecotoxicology and Environmental Safety*, **232**: 113223.

Jiang T, Xu Y X, Li Y et al. 2014. Seasonal dynamics of *Alexandrium tamarense* and occurrence of paralytic shellfish poisoning toxins in bivalves in Nanji Islands, East China Sea. *Marine and Freshwater Research*, **65**(4): 350-358, https://doi.org/10.1071/MF13001.

Kim Y O, Choi J, Baek S H et al. 2020. Tracking *Alexandrium catenella* from seed-bed to bloom on the southern coast of Korea. *Harmful Algae*, **99**: 101922, https://doi.org/10.1016/j.hal.2020.101922.

Kremp A, Lindholm T, Dreßler N et al. 2009. Bloom forming *Alexandrium ostenfeldii* (Dinophyceae) in shallow waters of the Åland Archipelago, Northern Baltic Sea. *Harmful Algae*, **8**(2): 318-328, https://doi.org/10.1016/j.hal.2008.07.004.

Lin Y T, Jia X P, Yang M L et al. 1999. Paralytic shellfish poison in contaminated shellfish along coast of China. *Tropic Oceanology*, **18**(1): 90-96. (in Chinese with English abstract)

Lionard M, Muylaert K, Tackx M et al. 2008. Evaluation of the performance of HPLC-CHEMTAX analysis for determining phytoplankton biomass and composition in a turbid estuary (Schelde, Belgium). *Estuarine*, *Coastal and Shelf Science*, **76**(4): 809-817, https://doi.org/10.1016/j.ecss.2007.08.003.

Liu Y, Yu R C, Kong F Z et al. 2017. Paralytic shellfish toxins in phytoplankton and shellfish samples collected from the Bohai Sea, China. *Marine Pollution Bulletin*, **115**: 324-331, https://doi.org/10.1016/j.marpolbul.2016.12.023.

Lu L, Jiang T, Xu Y et al. 2018. Succession of phytoplankton functional groups from spring to early summer in the central Bohai Sea using HPLC-CHEMTAX approaches. *Journal of Oceanography*, **74**(4): 381-392, https://doi.org/10.1007/s10872-018-0469-x.

Mackey M D, Mackey D J, Higgins H W et al. 1996. CHEMTAX — a program for estimating class abundances from chemical markers: application to HPLC measurements of phytoplankton. *Marine Ecology Progress Series*, **144**: 265-283, https://doi.org/10.3354/meps144265.

Maguer J F, Wafar M, Madec C et al. 2004. Nitrogen and phosphorus requirements of an *Alexandrium minutum* bloom in the Penzé Estuary, France. *Limnology and Oceanography*, **49**(4): 1108-1114, https://doi.org/10.4319/lo.2004.49.4.1108.

McGillicuddy D J Jr, Brosnahan M L, Couture D A et al. 2014. A red tide of *Alexandrium fundyense* in the Gulf of Maine. *Deep Sea Research Part II*: *Topical Studies in Oceanography*, **103**: 174-184.

Mendes C R B, Kerr R, Tavano V M et al. 2015. Cross-front phytoplankton pigments and chemotaxonomic groups in the Indian sector of the Southern Ocean. *Deep Sea Research Part II*: *Topical Studies in Oceanography*, **118**: 221-232, https://doi.org/10.1016/j.dsr2.2015.01.003.

Miranda-Alvarez C, González-Silvera A, Santamaría-Del-angel E et al. 2020. Phytoplankton pigments and community structure in the northeastern tropical pacific using HPLC-CHEMTAX analysis. *Journal of Oceanography*, **76**(2): 91-108, https://doi.org/10.1007/s10872-019-00528-3.

Nisbet I C. 1983. Paralytic shellfish poisoning: effects on breeding terns. *The Condor*, **85**(3): 338-345, https://doi.org/10.2307/1367071.

Nishitani L, Chew K. 1988. PSP toxins in the Pacific coast states: monitoring programs and effects on bivalve industries. *Journal of Shellfish Research*, **7**(4): 653-669.

Not F, Latasa M, Marie T et al. 2004. A single species, *Micromonas pusilla* (Prasinophyceae), dominates the eukaryotic picoplankton in the western English Channel. *Applied and Environmental Microbiology*, **70**(7): 4064-4072, https://doi.org/10.1128/AEM.70.7.4064-4072.2004.

Ou L J, Cai Y Y, Jin W Y et al. 2018. Understanding the nitrogen uptake and assimilation of the Chinese strain of *Aureococcus anophagefferens* (Pelagophyceae). *Algal Research*, **34**: 182-190, https://doi.org/10.1016/j.algal.2018.07.019.

Pan H Z, Li A F, Cui Z G et al. 2020. A comparative study of phytoplankton community structure and biomass determined by HPLC-CHEMTAX and microscopic methods during summer and autumn in the central Bohai Sea, China. *Marine Pollution Bulletin*, **155**: 111172, https://doi.org/10.1016/j.marpolbul.2020.111172.

Parsons T R, Harrison P J, Waters R. 1978. An experimental simulation of changes in diatom and flagellate blooms. *Journal of Experimental Marine Biology and Ecology*, **32**(3): 285-294, https://doi.org/10.1016/0022-0981(78)90122-3.

Pei S F, Laws E A, Zhu Y X et al. 2019. Nutrient dynamics and their interaction with phytoplankton growth during autumn in Liaodong Bay, China. *Continental Shelf Research*, **186**: 34-47, https://doi.org/10.1016/j.csr.2019.07.012.

Peng S T. 2015. The nutrient, total petroleum hydrocarbon and heavy metal contents in the seawater of Bohai Bay, China: Temporal-spatial variations, sources, pollution statuses, and ecological risks. *Marine Pollution Bulletin*, **95**(1): 445-451, https://doi.org/10.1016/j.marpolbul.2015.03.032.

Persich G R, Kulis D M, Lilly E L et al. 2006. Probable origin and toxin profile of *Alexandrium tamarense* (Lebour) Balech from southern Brazil. *Harmful Algae*, **5**(1): 36-44, https://doi.org/10.1016/j.hal.2005.04.002.

Pujari L, Wu C, Kan J J et al. 2019. Diversity and spatial distribution of chromophytic phytoplankton in the Bay of Bengal revealed by RuBisCO Genes (*rbc*L). *Frontiers in Microbiology*, **10**: 1501, https://doi.org/10.3389/fmicb.2019.01501.

Raposo M, Botelho M J, Costa S T et al. 2020. A carbamoylase-based bioassay for the detection of paralytic shellfish poisoning toxins. *Sensors*, **20**(2): 507, https://doi.org/10.3390/s20020507.

Reynolds C S. 2006. Ecology of phytoplankton. Cambridge University Press, New York, America. p.1-36.

Sarthou G, Timmermans K R, Blain S et al. 2005. Growth physiology and fate of diatoms in the ocean: a review. *Journal of Sea Research*, **53**(1-2): 25-42, https://doi.org/10.1016/j.seares.2004.01.007.

Seoane S, Garmendia M, Revilla M et al. 2011. Phytoplankton pigments and epifluorescence microscopy as tools for ecological status assessment in coastal and estuarine waters, within the Water Framework Directive. *Marine Pollution Bulletin*, **62**(7): 1484-1497, https://doi.org/10.1016/j.marpolbul.2011.04.010.

Shumway S E, Sherman-Caswell S, Hurst J W et al. 1988. Paralytic shellfish poisoning in Maine: monitoring a monster. *Journal of Shellfish Research*, **7**(4): 643-652.

Strickland J D H, Parsons T R. 1972. Determination of phosphorus. *In*: Strickland J D H eds. A Practical Handbook of Seawater Analysis. 2nd edn. Fisheries Research Board of Canada. Press, Ottawa, Canada. p. 123-124.

Townsend D W, Pettigrew N R, Thomas A C. 2001. Offshore blooms of the red tide dinoflagellate, *Alexandrium* sp., in the Gulf of Maine. *Continental Shelf Research*, **21**(4): 347-369, https://doi.org/10.1016/S0278-4343(00)00093-5.

Utermöhl H. 1958. Methods of collecting plankton for various purposes are discussed. *SIL Communications*, *1953-1996*, **9**(1): 1-38, https://doi.org/10.1080/05384680.1958.11904091.

Vila M, Camp J, Garcés E et al. 2001. High resolution spatio-temporal detection of potentially harmful dinoflagellates in confined waters of the NW Mediterranean. *Journal of Plankton Research*, **23**(5): 497-514, https://doi.org/10.1093/plankt/23.5.497.

Wang L H, Ou L J, Huang K X et al. 2018. Determination of the spatial and temporal variability of phytoplankton community structure in Daya Bay via HPLC-CHEMTAX pigment analysis. *Chinese Journal of Oceanology & Limnology*, **36**(3): 750-760, https://doi.org/10.1007/s00343-018-7103-z.

Wasmund N, Tuimala J, Suikkanen S et al. 2011. Long-term trends in phytoplankton composition in the western and central Baltic Sea. *Journal of Marine Systems*, **87**(2): 145-159, https://doi.org/10.1016/j.jmarsys.2011.03.010.

Wells M L, Karlson B, Wulff A et al. 2020. Future HAB science: directions and challenges in a changing climate. *Harmful Algae*, **91**: 101632, https://doi.org/10.1016/j.hal.2019.101632.

Wright S W, Van Den Enden R L, Pearce I et al. 2010. Phytoplankton community structure and stocks in the Southern Ocean (30-80°E) determined by CHEMTAX analysis of HPLC pigment signatures. *Deep Sea Research Part II*: *Topical Studies in Oceanography*, **57**(9-10): 758-778, https://doi.org/10.1016/j.dsr2.2009.06.015.

Xu S S, Song J M, Li X G et al. 2010. Changes in nitrogen and phosphorus and their effects on phytoplankton in the Bohai Sea. *Chinese Journal of Oceanology and Limnology*, **28**(4): 945-952, https://doi.org/10.1007/s00343-010-0005-3.

Xu X, Yu Z M, He L Y et al. 2017. Nano- and microphytoplankton community characteristics in brown tide bloom—prone waters of the Qinhuangdao coast, Bohai Sea, China. *Science China Earth Sciences*, **60**(6): 1189-1200, https://doi.org/10.1007/s11430-017-9036-0.

Yan G W, Jiang T, Zhang Y Y et al. 2020. Determining temporal and spatial distribution of autotrophic picoplankton community composition through HPLC-pigment method and flow cytometry in the central Bohai Sea (China). *Marine Pollution Bulletin*, **157**: 111261, https://doi.org/10.1016/j.marpolbul.2020.111261.

Yang J R, Pick F R, Hamilton P B. 1996. Changes in the planktonic diatom flora of a large mountain lake in response to fertilization. *Journal of Phycology*, **32**(2): 232-243, https://doi.org/10.1111/j.0022-3646.1996.00232.x.

Yang S M, Dong S G. 2006. Illustrations of Common Planktonic Diatoms in Chinese Seas. China Ocean University Press, Qingdao, China. 267p. (in Chinese)

Yang S M, Li R X, Dong S G. 2019. Dinoflagellates in the China's Seas III (Peridiniales). Ocean Press, Beijing, China. 211p. (in Chinese)

Yu R C, Zhang Q C, Liu Y et al. 2021. The dinoflagellate *Alexandrium catenella* producing only carbamate toxins may account for the seafood poisonings in Qinhuangdao, China. *Harmful Algae*, **103**: 101980, https://doi.org/10.1016/j.hal.2021.101980.

Zapata M, Rodríguez F, Garrido J L. 2000. Separation of chlorophylls and carotenoids from marine phytoplankton: a new HPLC method using a reversed phase C_8 column and pyridine-containing mobile phases. *Marine Ecology Progress Series*, **195**(3): 29-45, https://doi.org/10.3354/meps195029.

Zhai H C, Ning X R, Tang X X et al. 2011. Phytoplankton pigment patterns and community composition in the northern South China Sea during winter. *Chinese Journal of Oceanology and Limnology*, **29**(2): 233-245, https://doi.org/10.1007/s00343-011-0111-x.

Zhang J, Yu Z G, Raabe T et al. 2004. Dynamics of inorganic nutrient species in the Bohai seawaters. *Journal of Marine Systems*, **44**(3-4): 189-212, https://doi.org/10.1016/j.jmarsys.2003.09.010.

Zhang X, Xu X F, Dai Y Y et al. 2018. Phytoplankton community characteristics and variation at artificial reefs of Tianjin offshore. *Progress in Fishery Sciences*, **39**(6): 1-10. (in Chinese with English abstract)

Zhang Y Y. 2020. Source Analysis and Forecasting Technology of Paralytic Shellfish Toxins in Mussels Culture Area of Qinhuangdao. Jiangsu Ocean University, Lianyungang. p.40-52. (in Chinese with English abstract)

Zhou M J, Shen Z L, Yu R C. 2008. Responses of a coastal phytoplankton community to increased nutrient input from the Changjiang (Yangtze) River. *Continental Shelf Research*, **28**(12): 1483-1489, https://doi.org/10.1016/j.csr.2007.02.009.